Journal of Chromatography A, 1218 (2011) 1861–1877

Contents lists available at ScienceDirect

Journal of Chromatography A

journal homepage: www.elsevier.com/locate/chroma

Developing a validated liquid chromatography–mass spectrometric method for the simultaneous analysis of five bioactive quassinoid markers for the standardization of manufactured batches of *Eurycoma longifolia* Jack extract as antimalarial medicaments

Chin-Hoe Teh, Vikneswaran Murugaiyah, Kit-Lam Chan*

School of Pharmaceutical Sciences, Universiti Sains Malaysia, 11800 Penang, Malaysia

ARTICLE INFO

Article history:
Received 30 November 2010
Received in revised form 26 January 2011
Accepted 5 February 2011
Available online 13 February 2011

Keywords:
Simaroubaceae
Eurycoma longifolia
Quassinoids
LC–MS analysis
Standardized extracts

ABSTRACT

An extensive comparative study on the electrospray ionization (ESI) and atmospheric pressure chemical ionization (APCI) mass spectrometry using automated flow injection analysis (FIA), was performed on eurycomanone (**1**), 13α(21)-epoxyeurycomanone (**2**), eurycomanol (**3**), eurycomanol-2-*O*-β-D-glucopyranoside (**4**), and 13,21-dihydroeurycomanone (**5**), the bioactive markers isolated from *Eurycoma longifolia*. The effects of eluent mixture (methanol or acetonitrile in water) and acidic modifiers (acetic acid, formic acid and trifluoroacetic acid) on the ionization efficiency of the markers were also investigated. The ESI in the positive ion mode with methanol containing 0.1% (v/v) acetic acid was selected for the subsequent optimization of nebulizer pressure, dry gas flow, dry gas temperature and capillary voltage to improve the sensitivity of the total ion chromatogram (TIC). Fragmentation of the analytes was further investigated by varying the capillary exit offset voltage and fragmentation amplitude in positive mode of ESI. The detection limits (LODs) were determined in isolation mode (selected ion monitoring, SIM). Their limits of detection (LODs) ranged between 0.03 and 0.1 $\mu g\,mL^{-1}$ while the intra-day and inter-day precisions were less than 5.72% and 4.82%, respectively. The method was next applied for the simultaneous analysis of the markers to standardize various batches of manufactured extracts of *E. longifolia* for potential use as antimalarial products. Multiple Reaction Monitoring (MRM) mode was used for the quantification of analytes which gave protonated molecular ion, $[M+H]^+$. For those without pseudo-molecular ions, SIM mode was used to quantify the analytes. The batches contained 5.65–9.95% of eurycomanone (**1**), 5.21–19.75% of eurycomanol (**3**) and 7.59–19.95% of eurycomanol-2-*O*-β-D-glucopyranoside (**4**) as major quassinoids whereas, 13α(21)-epoxyeurycomanone (**2**), and 13,21-dihydroeurycomanone (**5**) were much lower in concentrations of 0.78–3.90% and 0.47–1.76%, respectively.

1. Introduction

The mass spectrometry (MS) has become popular as a versatile and specific detection method in liquid chromatography (LC), especially for the analysis of multiple components in herbal and pharmaceutical products [1,2]. LC–MS is also recognized as a powerful tool for identification and quantification of various classes of natural product constituents [3–6]. From the plant kingdom, quassinoids are bitter constituents found exclusively in various species of the *Simarouboidaea* (subfamily of Simaroubaceae) and are biogenetically degraded triterpenes displaying a wide range of physiological properties *in vitro* and/or *in vivo* [7–9]. Hitherto, only three reports are available on the phytochemical analysis of quassinoids using mass spectrometry [10–12]. No extensive MS optimization and fragmentation studies on the quassinoids have been reported previously. Nevertheless, numerous reports are available on LC methods for the analysis of quassinoids using UV, photodiode array or fluorescence detections. However, these methods were not sensitive to detect non-chromophoric bioactive constituents, named eurycomanol (**3**) and eurycomanol-2-*O*-β-D-glucopyranoside (**4**) present in *Eurycoma longifolia* [13–15]. Thus, the present study developed and optimized a HPLC method using ESI and APCI in positive and negative ion modes for the simultaneous determination of five quassinoid markers, eurycomanone (**1**), 13α(21)-epoxyeurycomanone (**2**), eurycomanol (**3**), eurycomanol-2-*O*-β-D-glucopyranoside (**4**), and 13,21-dihydroeurycomanone (**5**) (Fig. 1). The method was then validated and later extended to standardize various batches of *E. longifolia* extracts manufactured for antimalarial activity [16].

* Corresponding author. Tel.: +60 4 6532696; fax: +60 4 6576836.
E-mail addresses: kitlamc@gmail.com, klchan@usm.my (K.-L. Chan).

0021-9673/$ – see front matter © 2011 Elsevier B.V. All rights reserved.
doi:10.1016/j.chroma.2011.02.014

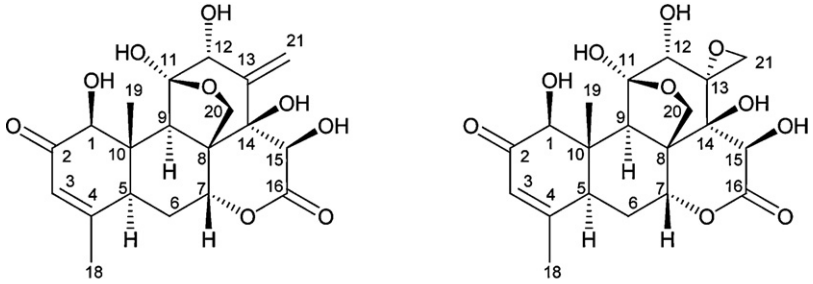

Eurycomanone **(1)**

13α(21)-Epoxyeurycomanone **(2)**

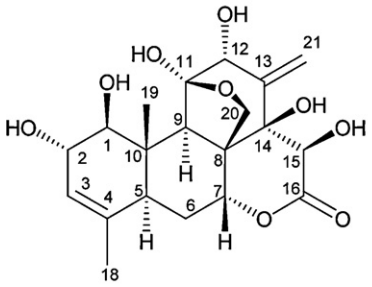

Eurycomanol **(3)**

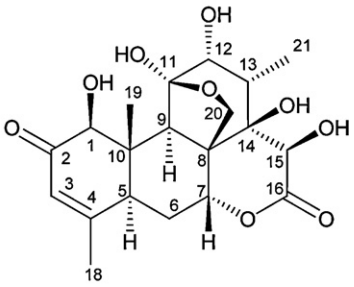

13,21-Dihydroeurycomanone **(5)**

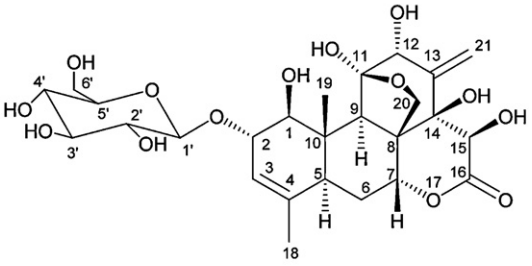

Eurycomanol-2-*O*-β-D-glucopyranoside **(4)**

Fig. 1. The structures of the isolated compounds.

2. Material and methods

2.1. Chemicals and reagents

The analytical grade solvents (ethyl acetate, *n*-butanol, chloroform, *n*-hexane, absolute ethanol and methanol) and HPLC grade methanol and acetonitrile were purchased from Merck (Darmstadt, Germany). Deionized water for chromatography was prepared in-house using Maxima ultra pure water purifier system (Elgastat; Bucks, England). Resins of styrene and divinylbenzene (Diaion HP 20) were purchased by Mitsubishi (Tokyo, Japan). Silica gel No. 7734, 9385 and 60 PF_{254} containing gypsum (No. 7749) were purchased from Merck (Darmstadt, Germany). Acetic acid, formic acid and trifluoroacetic acid were purchased from R & M Essex Chemicals (UK), Fluka and Sigma–Aldrich (Germany), respectively. HPLC solvents were passed through a 0.45 μm nylon membrane filter (Whatman, UK) before use.

2.2. Extraction and isolation of reference compounds

2.2.1. Plant materials

The root samples of *E. longifolia* were purchased from Hovid Berhad, Ipoh, Malaysia. The plant was authenticated by Professor Ahmad Latif from the National University of Malaysia and a voucher specimen (No. 785-117) was deposited in the Penang Botanical Garden, Penang, Malaysia.

2.2.2. Preparation of the standards

The powdered roots of *E. longifolia* (11.6 kg) were extracted with 6× 4 L of 95% MeOH for 6 days at 60 °C. The combined MeOH extract on evaporation to dryness yielded 485 g of dark brown residue which was next chromatographed on a Diaion HP 20 column using H_2O–MeOH (1:0–0:1) gradient mixtures to afford 4 fractions (Fr 1–4). Fr 2 was concentrated under *vacuo* to give 52.2 g of residue. The residue was suspended in water and partitioned successively with ethyl acetate and saturated *n*-butanol to yield three sub-fractions of ethyl acetate, *n*-butanol and water. Detailed purification and isolation methods to yield the reference compounds are given in Supplementary material 1.

These isolated compounds were used as markers for the optimization, validation and quantification of the chemical constituents of various manufactured extracts of *E. longifolia*. The LC–ESI-MS purity check was performed using an Agilent 1100 series LC–MSD Trap G2445 VL (Agilent Technologies, Palo Alto, CA, USA) HPLC system and all the markers were at least 96% pure. The structures of the isolated compounds were established primarily

by interpretation of conventional spectroscopic data, such as IR, UV, NMR spectroscopy and were further confirmed by direct comparison of their physicochemical and NMR data with those in the literature [17–19].

2.3. Optimization of LC and MS conditions

2.3.1. Preparation of the MS optimization standards

For optimization of MS conditions, stock solutions of 100 mg L^{-1} were prepared by accurately weighing each marker, then dissolving it in methanol and stored at 4 °C. Working solutions were prepared by diluting an aliquot of the stock solution with the mobile phase to a concentration of 10 mg L^{-1}. All the diluted solutions were filtered through a 0.45 μm PTFE syringe filter (Whatman, UK) prior to injection into the LC system.

2.3.2. LC–MS

An Agilent 1100 series LC–MSD Trap G2445 VL (Agilent Technologies, Palo Alto, CA, USA) was used for the analysis. The system consists of an autosampler, a degasser unit, a binary solvent pump, and a diode array UV–Vis detector coupled in series with an ion trap mass selective detector (MSD). The MSD consisted of an atmospheric pressure ionization (API) source configured to either atmospheric pressure chemical ionization (APCI) or electrospray ionization (ESI) interface. The LC–MSD system was controlled by LC–MSD Trap software, version 5.2 (Agilent Technologies, Palo Alto, CA, USA), and data acquisition was analyzed, on a computer equipped with Agilent Chemstation software, version A. 10.02.

For optimization of LC conditions, an Inertsil ODS-3 column of 2.1 mm × 50 mm and 3 μm particle size (GL Sciences Inc., Tokyo, Japan) preconnected with an ODS-3, 7 μm particle size, 1.5 mm × 10 mm cartridge guard column (GL Sciences Inc., Tokyo, Japan) was used. The injection volume was 5 μL, the flow-rate was 300 μL min^{-1} and the run-time was 60 min using ESI interface. In order to identify the main ion signals produced by each analyte, an automated Flow Injection Analysis (FIA) was performed and provided a rapid evaluation of individual MS parameters on the ion signals of the five biomarkers. A 5 μL of the reference compound was consecutively injected three times directly into the MSD without passing through the separation column when performing FIA analysis.

The Ion Charge Control (ICC) target value and the Maximum Accumulation Time were set as 50,000 and 100.00 ms, respectively, according to the manufacturer's instructions. Rolling averaging was turned off during the analysis. The trap drive was set at 60.0 for the flow injection analysis. Compound stability was set at 90% and the normal optimized mode was used for target analysis. The initial mass spectrometer detector (MSD) conditions for ESI probe as suggested in the Operation Manual of LC/MSD Trap System Overview VL and SL Models from Agilent Technologies were followed. The MS parameters included 350 °C of dry gas temperature, 8 L min^{-1} of dry gas flow, 30 psi of nebulizer pressure and −3500 V of capillary voltage.

2.3.3. Optimization of MS conditions

Extensive compound-oriented MS optimizations were performed on the five quassinoids and were summarized in Supplementary materials 2 and 3. Two organic solvents commonly used as components of the mobile phase were methanol and acetonitrile, used alone or in combination with water and in the absence/presence of organic modifier such as formic acid, acetic acid or trifluoroacetic acid, were tested for each compound. Each analyte, at a concentration of 10 mg L^{-1} with an injection volume of 5 μL, was injected into the flow of the isocratic mobile phase at 300 μL min^{-1} using FIA. Three replicates were performed for the evaluation of MS response for each compound. The mass spectra were obtained in full scan mode with range of *m/z* 50–700 and the optimum conditions were selected based on the MS signals reported in the form of peak areas of the total ion chromatograms (TIC) produced for the analyte of interest. FIA experiments were also performed in both positive and negative modes and subsequently, a decision was made to select the ionization mode for study. In choosing the best ionization mode, the main criterion was the high MS response in combination with high sensitivity (signal-to-noise ratio) of each analyte.

The FIA experiments on mobile phase compositions (with and without the ionizing agents) and on ion mode selections were repeated for the compounds of interest using APCI interface. Comparison of APCI and ESI interfaces was then carried out. Similarly, the preliminary MSD conditions for APCI probe suggested in the Operation Manual of LC/MSD Trap System Overview VL and SL Models from Agilent Technologies, including, 350 °C of dry gas temperature, 7 L min^{-1} of dry gas flow, 60 psi of nebulizer pressure and −3500 V of capillary voltage were used to detect the analytes in FIA. Apart from aforementioned parameters, corona current and vaporizer temperature, characteristic for APCI interface were preset as 4000 nA and 300 °C, respectively, for positive mode of APCI and 10,000 nA and 300 °C, respectively, for negative mode of APCI in the preliminary FIA analysis.

2.3.4. Re-optimization of liquid chromatographic conditions with addition of acetic acid

In order to further confirm the effects of eluent composition (with the addition of the ionizing agents to mobile phase) on the MS response of the analytes, the isocratic mobile phase consisted of water–acetonitrile (96:4) – 0.1% acetic acid (v/v) and water–methanol (91:9) – 0.1% acetic acid (v/v), with a flow-rate of 300 μL min^{-1} and run time of 60 min were evaluated in both positive and negative mode of ESI and positive mode of APCI. Subsequently, the influence of the acetic acid (0.1, 0.2, 0.3, 0.4 and 0.5%, v/v) on the positive ion of ESI-MS detections and chromatographic retention times of the analytes was also investigated.

2.3.5. Nebulizer pressure, dry gas flow, dry gas temperature, and capillary voltage on positive mode of ESI-MS response

Optimization of interface parameters of ESI was performed using FIA analysis. Each analyte, at a concentration of 10 mg L^{-1} and an injection volume of 5 μL, was injected into ESI positive ion mode with the flow of water–methanol (91:9) – 0.1% acetic acid (v/v) mobile phase at 300 μL min^{-1}. Three replicates were performed for the evaluation of TIC-MS response for each compound. The nebulizing pressure was varied from 30 to 60 psi and the drying gas flow rate was varied between 6 and 12 L min^{-1}. In addition, the dry gas temperature was tested between 250 and 350 °C while the capillary voltage was tested between 2.5 and 4.5 kV. Under the above conditions, the mass spectra were obtained in full scan mode with range of *m/z* 50–700.

2.3.6. Capillary exit offset on ionization patterns of the analytes in ESI

13α(21)-Epoxyeurycomanone (**2**) and 13,21-dihydroeurycomanone (**5**) readily formed the pseudo-molecular ions, $[M+H]^+$ in ESI positive mode. The highest intensity of the $[M+H]^+$ ion of 11 and 15 were obtained by varying the capillary exit offset voltage (+10 to +210 V). Eurycomanone (**1**), eurycomanol (**3**) and eurycomanol-2-*O*-β-D-glucopyranoside (**4**), however, did not gave the protonated molecules $[M+H]^+$ in the electrospray interface. These quassinoids only produced the $[M+H-H_2O]^+$, $[M+H-2H_2O]^+$, and $[M+H-C_6H_{12}O_6-2H_2O]^+$ fragments as the most abundant ions of **1**, **3** and **4**, respectively. By varying the capillary exit offset from +10 V to +210 V, the maximum intensity of these ions was obtained. All the FIA experiments were performed

Table 1
Ion isolation and MS/MS or MRM detection modes.

Compound	Isolation (*m/z*)	MS/MS or MRM (*m/z*)
Eurycomanone (**1**)	391.3 $[M+H-H_2O]^+$	391.3 → 251.1, 279.1
13α (21)-Epoxyeurycomanone (**2**)	425.2 $[M+H]^+$	425.2 → 407.1
Eurycomanol (**3**)	375.2 $[M+H-2H_2O]^+$	375.2 → 281.1, 255.2
Eurycomanol-2-*O*-β-D-glucopyranoside (**4**)	375.2 $[M+H-C_6H_{12}O_6-2H_2O]^+$	375.2 → 281.1, 255.2
13,21-Dihydroeurycomanone (**5**)	411.2 $[M+H]^+$	411.2 → 393.2

in triplicate in the ESI positive mode and the mass spectra were obtained in full scan mode (*m/z* 50–700).

2.3.7. Effect of fragmentation amplitude on the precursor ion in ESI

In order to optimize the yield of the daughter ions from the precursor ion for each of the analytes, fragmentation amplitude was varied between 0.8 V and 1.5 V. The fragmentation delay, fragmentation time and fragmentation width were set as 0 ms, 40 ms and 10 *m/z*, respectively, as default values. A mass width of 4.0 was used in order to specify the ion monitored and during the mass spectrometry–mass spectrometry (MS/MS) or multiple reaction monitoring (MRM) scanning mode the same width was utilized for both the precursor and the product ion selection. If there was no protonated molecular ion, $[M+H]^+$ formed, then the fragment ion with the highest intensity (base peak) was use for further quantification. The ions monitored in MS operation with isolation and MS/MS or MRM mode are shown in Table 1.

2.4. Method validation

2.4.1. Sensitivity and limits of detection (LOD)

The detection limits were studied to investigate the sensitivity of the method developed. The LOD of an analyte is the lowest concentration which yields an instrumental signal significantly different from the background signal at a signal-to-noise (S/N) ratio of 3. For the determination of LOD, 1 mg mL^{-1} of the standard solution of analyte was serially diluted with the mobile phase and was then injected into the system. Each individual standard at a certain concentration was consecutively injected three times.

2.4.2. Preparation of the calibration standards

For the method validation and LC–ESI-MS quantitative analysis studies, standard stock solutions were prepared by accurately weighing 1 mg of the analyte and dissolving it in 1 mL of methanol. Working solutions were daily prepared prior to use by diluting an aliquot of the stock solution in the mobile phase. Working solutions were prepared for eurycomanone (**1**) at 0.5, 1.0, 5.0, 10.0 and 20 μg mL^{-1}, for 13α(21)-epoxyeuryromanone (**2**), eurycomanol (**3**), and 13,21-dihydroeurycomanone (**5**) at concentrations of 0.5, 5.0, 10.0, 25.0 and 30.0 μg mL^{-1}, and for eurycomanol-2-O-β-D-glucopyranoside (**4**) at 1.0, 5.0, 10.0, 20.0 and 30.0 μg mL^{-1}. The stock and calibration standards were stored at −20 °C prior to use. Freshly prepared working standards were used to construct the calibration curves daily for the determination of recovery, inter-day and intra-day precision and accuracy of the method. No internal standard was added. Time segments were utilized to study an individual component parent ion (isolation) or parent-to-product ion transition (MS/MS or MRM) individually at specific time points during analyses.

Data acquisition during the chromatographic separations was from the following modes:

(i) Isolation mode using selected ion monitoring (SIM) was used to monitor from 7.8 to 11.5 min for eurycomanone (**1**) (*m/z* 391.3); from 23.0 to 36.0 min for eurycomanol (**3**) (*m/z* 375.2); and from 36.0 to 49.0 min for eurycomanol-2-O-β-D-glucopyranoside (**4**) (*m/z* 375.2).
(ii) Multiple reaction monitoring mode (MRM) was selected to monitor from 0 to 7.8 min for 13α(21)-epoxyeuryromanone (**2**) (transition from *m/z* 425.2 to 407.1); and from 11.5 to 13.5 min for 13,21-dihydroeurycomanone (**5**) (transition from *m/z* 411.2 to 393.2).

2.4.3. Limits of quantification (LOQ), calibration curves and linearity ranges

The linear dynamic ranges of the LC–MS method for the determination of the five biomarker analytes were evaluated from a set of five solutions, at concentrations ranging from 0.5 to 30 μg mL^{-1}. Each individual standard at a fixed concentration was consecutively injected three times. The calibration curves were constructed by plotting peak areas against the analyte concentrations prepared. Linear regression analysis was also performed for each reference standard and the linearity was expressed as the squared correlation coefficient (r^2). The lowest concentration at the linear range is the limit of quantification (LOQ). The LOQ was determined by triplicate analysis of a series of decreasing concentrations of standard solutions. The concentration level that gave the signal-to-noise ratio of 10 was reported as the LOQ value.

2.4.4. Precision and accuracy

The precision was expressed as the relative standard deviation (% RSD) at a concentration level used, whereas accuracy was expressed as percentage of true value. The intra-day precision and accuracy were evaluated on column for each analyte by injecting the same standard solution five times in a single day. The inter-day precision and accuracy were assessed on column by analyzing the same standard solution over five consecutive days.

2.4.5. Recovery studies

The recovery experiment was carried out by addition method. A series of bioactive extracts at a concentration of 50 μg mL^{-1} were prepared and then spiked with three standard solutions of increasing concentration (final concentration in the mixture 0.50, 5.00 and 20.00 μg mL^{-1}). The bioactive extracts at 50 μg mL^{-1} served as the base matrix and contained very low amount of the standards. After addition of standard solutions, the samples were vortex-mixed and filtered through a 0.45 μm PTFE syringe filter (Whatman, UK). The samples were diluted accordingly prior to analysis. Samples were determined in triplicate. The % recovery of each quassinoid standard was calculated following the equation as previously reported [33].

2.5. Application of the validated LC–ESI-MS method for the simultaneous analysis of five quassinoids in bioactive extracts of *E. longifolia*

2.5.1. Preparation of the samples

The roots of *E. longifolia* were purchased from Hovid Berhad Malaysia. About 100 kg of the powdered roots were extracted in the accredited Good Manufacturing Practice (GMP) factory at Ipoh, Malaysia, in 3× 1000 L of methanol at 8 h per day for 5 days and the combined filtrate were then evaporated to dryness under partial vacuum. The dried residue (3% (w/w) of roots) was next

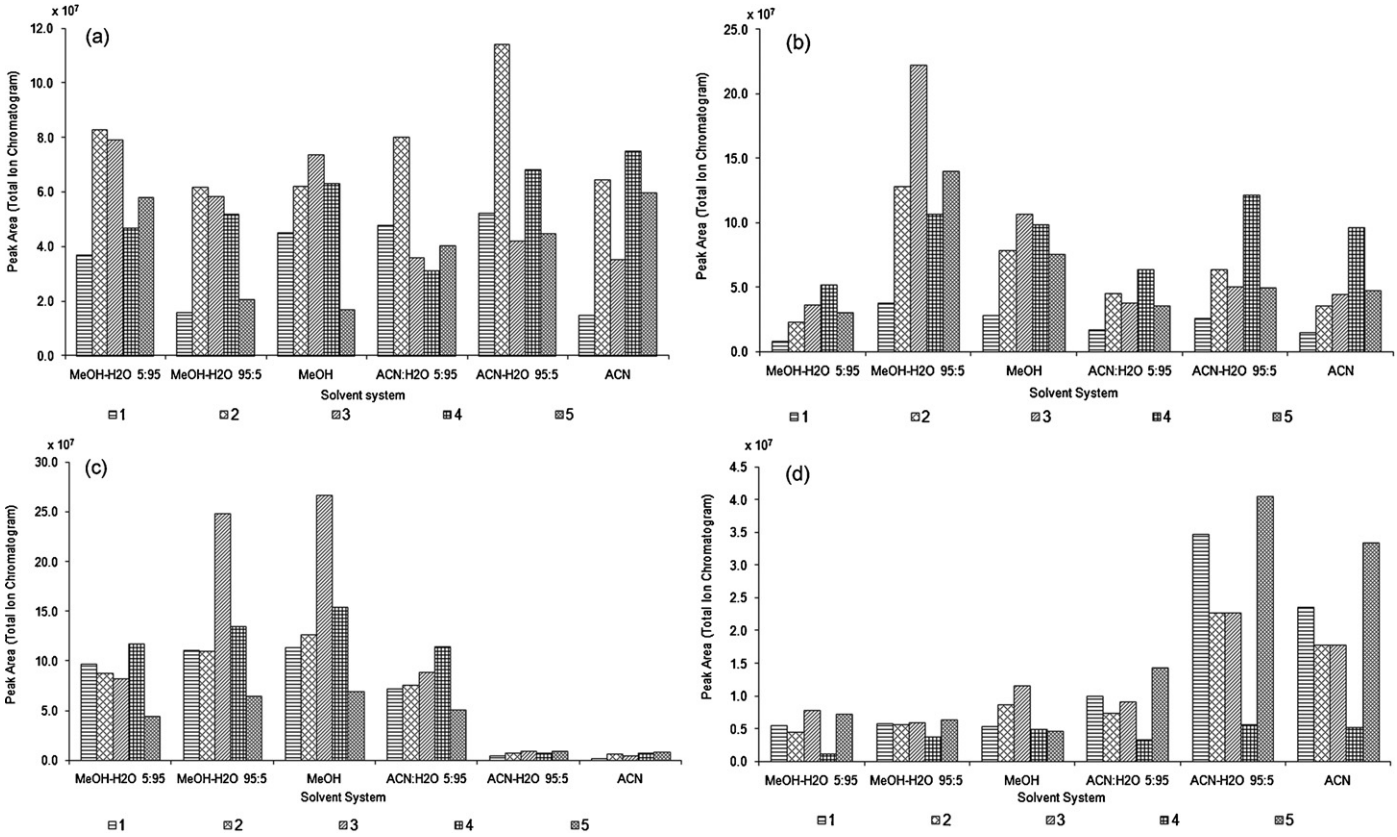

Fig. 2. Effect of LC-eluent on (a) positive mode ESI-MS signal, (b) negative mode ESI-MS signal, (c) positive mode APCI-MS signal, and (d) negative mode APCI-MS signal of five major *E. longifolia* quassinoids. Compound identification: eurycomanone (**1**), 13α(21)-epoxyeuryromanone (**2**), eurycomanol (**3**), eurycomanol-2-O-β-D-glucopyranoside (**4**) and 13,21-dihydroeurycomanone (**5**).

chromatographed following the procedure as previously described in Section 2.2.2 to yield the selected extract Fr 2 (10% (w/w) of residue). Six batches of *E. longifolia* extract Fr 2 were produced in the factory and each was subjected to the present LC–ESI-MS analysis. A Fr 2 sample was accurately weighed and dissolved in HPLC grade methanol to produce a stock solution of 1000 μg mL^{-1}. The stock solution was filtered through a 0.45 μm PTFE syringe filter (Whatman, UK) and then diluted to a concentration of 100 μg mL^{-1} with the mobile phase prior to use.

2.5.2. Quantitative determination of major quassinoids

A 5 μL of the diluted extract Fr 2 was injected into the HPLC column. The concentration and profile of eurycomanone (**1**), 13α(21)-epoxyeuryromanone (**2**), eurycomanol (**3**) eurycomanol-2-O-β-D-glucopyranoside (**4**), and 13,21-dihydroeurycomanone (**5**), in the extract were determined using optimized LC–ESI-MS parameters. Peak identifications were made by matching the retention times and the fragmentation patterns with those of the standard compounds, and were quantified using the external standard method.

3. Results and discussion

3.1. Optimization of mobile phase compositions on LC separation

Preliminary optimization of the LC conditions for a standard mixture of five quassinoids at 30 mg L^{-1} each indicated that the optimum mobile phases for the best separation of **1** and **5** were acetonitrile–water (4:96, v/v) and methanol–water (9:91, v/v), respectively. With the methanol–water mixture, the separation took a slightly longer time when compared to acetonitrile–water mixture, with total running time of 43.7 and 35.9 min, respectively.

3.2. Optimization of LC–API-MS parameters

The API mass spectrometer can be configured in APCI and ESI interfaces. Due to the difference in ionization mechanisms of APCI and ESI interfaces [20], the ionization characteristic and the sensitivity of the analyte in APCI and ESI may also vary [21]. Moreover, the ionization efficiency is compound-dependent parameter. Based on this idea, in the present study the five analytes were tested individually using both ESI and APCI techniques. It has also been reported that the selection of either positive or negative ionization mode may have a strong impact on the intensity of the MS signal [6]. Therefore, the API interfaces which can be operated in positive and negative mode were used to analyze the five analytes of *E. longifolia*. In addition, the results from the previous studies showed that eluent compositions have great effects on the ionization efficiency of analytes [6,21,22]. As a result, to evaluate the influence of organic modifiers on ESI-MS and APCI-MS response of all of the analytes, methanol and acetonitrile, being commonly used as API solvents, and mixtures of these solvents with water were evaluated. The MS responses of the analytes were expressed as peak areas of the total ion chromatograms (TIC) of the compounds of interest.

3.2.1. The influence of mobile phase composition on ESI-MS and APCI-MS response

Fig. 2a showed that acetonitrile and methanolic mobile phase gave almost similar responses for the tested analytes in the positive ion mode of ESI. Generally, there were no correlation between the MS response of the analytes and the mobile phase composi-

tions. For a 5% of organic solvent composition, methanol appears a more suitable solvent for positive ionization ESI-MS analysis of the compounds of interest than acetonitrile because it gave a slight improvement in ESI ionization efficiency compared with acetonitrile. Fig. 2b showed the influence of eluent composition on the peak areas of total ion chromatograms of analytes in the negative ionization mode of ESI. The ideal solvent based on chromatographic viewpoint favored the acetonitrile mobile phases over methanolic mobile phases as acetonitrile–water 5:95 gave a slightly higher ESI-MS response for the tested analytes as compared with methanol–water 5:95 ratio. As depicted in Fig. 2c, the MS response of the analytes was generally observed to be higher in methanol-based eluents than acetonitrile-based eluents when positive ion mode of APCI was used. For the organic solvent-H_2O (5:95) composition, with respect to methanol, substitution with acetonitrile in the eluent caused an increase in the signal intensity of **3** and **5** but a decrease in the MS signals of **1**, **2** and **4**. It has been reported that acetonitrile can be a good reagent gas for the ionization of medium polar analytes in negative APCI [23]. For quassinoids, acetonitrile work well as a reagent gas when used negative ionization APCI. As shown in Fig. 2d, varying the percentage of water in the CH_3OH–H_2O mixture did not show remarkable effects on the negative mode of APCI, however, decrease of water content in the acetonitrile mobile phase provided a slight increase in the sensitivity of the MS signal of the analytes. The acetonitrile–water eluent (5:95) seems to be a better eluent than methanol–water eluent (5:95) when the standards were analyzed using APCI negative mode due to the slightly higher sensitivity of the five analytes achieved.

3.2.2. The influence of acidic modifier on ESI-MS and APCI-MS response

Further investigations were performed on eluent with organic solvent: H_2O ratio of 5:95 on the basis of its suitability from chromatographic view point which allowed the baseline separation of the analytes in this study. As demonstrated in previous literature reports, the addition of acidic modifiers to the LC eluent has dramatic effects on the ionization of analytes and may substantially influence the sensitivity of API interface [21,22]. As a result, the API response of the analytes in mobile phases that contained methanol or acetonitrile, with or without formic acid, acetic acid and trifluoroacetic acid was investigated and compared. Generally, the responses of the analytes in positive ionization mode of ESI were found to be higher in the presence of acetic acid than in the presence of formic acid or trifluoroacetic acid. For both the methanolic and the acetonitrile mobile phases, the presence of acetic acid showed signal enhancement for most of the analytes, except for **2** which experienced some degree of ion suppression. In particular, the presence of acetic acid in the methanolic mobile phase significantly increased the positive ion responses of **1** by two-fold (Fig. 3b(i)), while in the acetonitrile mobile phase it significantly improved the ionization of **3** and **4** by three-fold (Fig. 3a(i)). As seen in Fig. 3a(i) and b(i), trifluoroacetic acid (TFA) showed considerably ion suppression for all the analytes of interest in positive ion mode of ESI when it was used as acidic modifier in acetonitrile and methanolic mobile phase.

Responses were generally observed to be lower in methanol than acetonitrile in the presence of the acidic modifiers when the analytes were analyzed with negative ion ESI-MS (Fig. 3a(ii) and b(ii)). In addition, all the analytes gave higher negative ion responses of ESI in the presence of acetic acid than in formic acid or trifluoroacetic acid when the total ion chromatograms were obtained in methanolic and acetonitrile mobile phases. Interestingly, the **4** gave a much higher negative ion responses than its aglycone, **3** in methanol and acetonitrile mobile phases, with or without formic acid, acetic acid or trifluoroacetic acid. For both methanolic and acetonitrile mobile phases, the presence of acetic acid significantly increased the negative ion responses of **1** by three-fold and two-fold, respectively. On the other hand, the negative ion responses of **5** in both methanolic and acetonitrile mobile phases were slightly suppressed in the presence of acetic acid. Signal suppression was also observed in the negative mode of ESI when **2** was analyzed using the acetonitrile mobile phase with the addition of 0.1% of acetic acid (Fig. 3a(ii)). With the exception of **1**, addition of 0.1% of formic acid to the methanolic and acetonitrile mobile phases decreased the signal intensity of the other five analytes in the negative ion mode of ESI. As seen in Fig. 3a(ii) and b(ii), the presence of trifluoroacetic acid in both methanolic and acetonitrile mobile phases significantly suppressed the negative ion responses of the analytes of interest.

The effect of acidic modifiers on the APCI-MS response was much less pronounced than in ESI-MS due mainly to the ionization process of APCI-MS involving the proton transfer by the gas phase ion [21]. However, as shown in Fig. 3a(iii) and b(iii), the addition of acidic modifiers to the methanolic and acetonitrile mobile phases have significantly suppressed the ionization of the analytes and yielded poor positive ion responses in APCI. Similarly, in negative APCI, the addition of formic acid and acetic acid caused remarkable decrease in the analytes response, and trifluoroacetic acid totally suppressed the ionization of the analytes and caused the complete loss of MS signal of all analytes in study (Fig. 3a(iv) and b(iv)).

3.2.3. Influence of mobile phase compositions on chromatographic separation and MS responses using positive mode of ESI and APCI

As the preliminary MS experiments were done using single compound without column separation, a mixed standard consisting of five marker compounds at a concentration of 30 mg L^{-1} each, was tested with chromatographic column. Although mobile phases based on acetonitrile–water mixtures gave lower column pressure and showed slightly shorter run times as compared to methanol, with total running time of 42.0 min and 50.0 min, respectively, methanol was chosen as one component of the mobile phase on the basis of higher MS responses produced by the analytes (data not shown). In addition, the quassinoids gave higher MS response in ESI positive mode than in negative mode. This result was in agreement with the FIA analysis. Moreover, positive ion mode of ESI gave a higher MS response for all of the analytes than in APCI positive ion mode. Hence, it can be concluded that the ESI positive mode is superior to APCI positive ion mode.

3.2.4. Influence of acetic acid concentration on chromatographic separation and MS responses using positive mode of ESI

Having selected the acidic modifier from the preliminary experiments, its concentration is also critical. By adjustment of the concentrations of acidic modifier, MS responses and retention times of the analytes could vary significantly [24]. Consequently, using the methanol–water (9: 91, v/v) as eluent, the influence of different percentages of acetic acid (0.1–0.5%, v/v) on the MS signal intensity and retention time of five compounds was studied. **4**, which was the last compound to elute, showed a retention time of 44.5 min and 29.4 min when water–methanol (91:9, v/v) + 0.1% acetic acid and water–methanol (91:9, v/v) + 0.5% acetic acid, respectively, were used as the mobile phase. Although high composition of acetic acid caused shorter total run times, increasing acetic acid content, in general, also lowered the intensity of the MS signals for all analytes (data not shown). Thus, the water–methanol (91:9, v/v) + 0.1% acetic acid was chosen as the mobile phase for the subsequent investigation on the basis of higher MS response of all analytes.

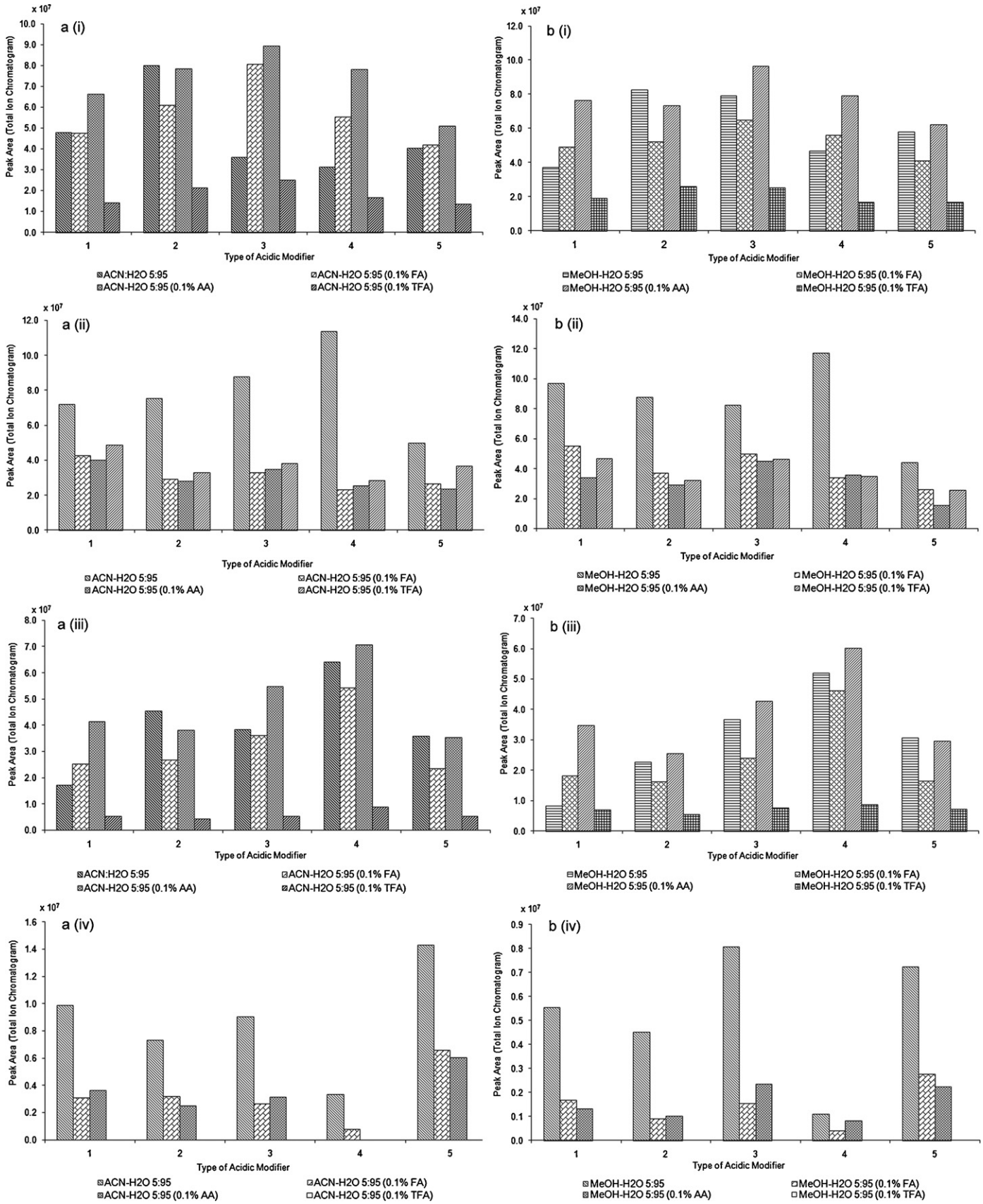

Fig. 3. Influence of acidic modifier in (a) ACN-based eluents, (b) MeOH-based eluents on ionization of five major quassinoids in (i) positive mode ESI, (ii) negative mode ESI, (iii) positive mode APCI, and (iv) negative mode APCI full scan MS signal. AA: Acetic acid; FA: Formic acid; TFA: Trifluoroacetic acid. Compound identification: eurycomanone (**1**), 13α(21)-epoxyeuryromanone (**2**), eurycomanol (**3**), eurycomanol-2-O-β-D-glucopyranoside (**4**) and 13,21-dihydroeurycomanone (**5**).

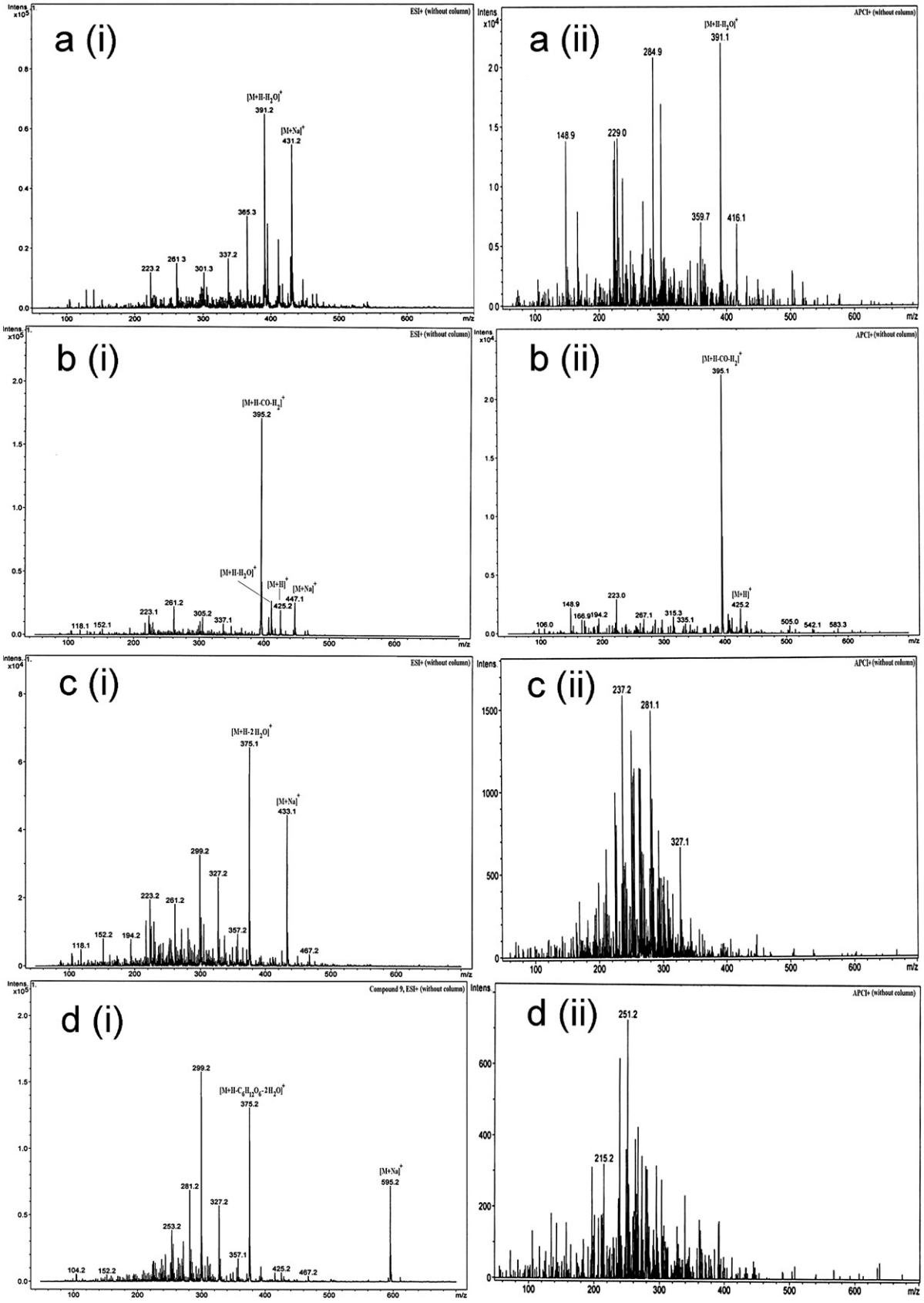

Fig. 4. Positive mode (i) ESI-MS and (ii) APCI-MS spectra of (a) eurycomanone (**1**), (b) 13α(21)-epoxyeurycomanone (**2**) and (c) eurycomanol (**3**), (d) eurycomanol-2-O-β-D-glucopyranoside (**4**) and (e) 13,21-dihydroeurycomanone (**5**) using FIA.

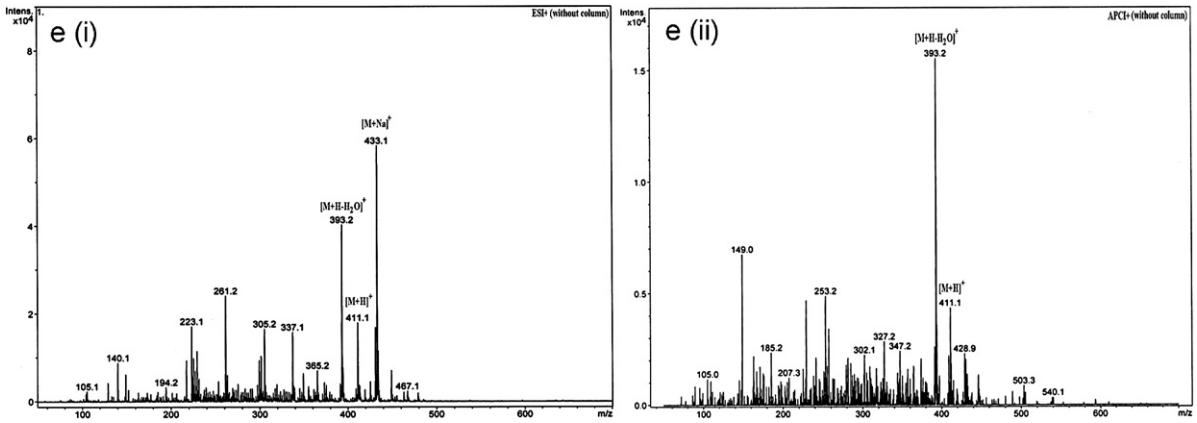

Fig. 4. (*Continued.*)

3.2.5. Ionization patterns of quassinoids in ESI and APCI

When making a choice between different interfaces and MS polarities for quantification purpose, the methodology development not only optimizes the detection sensitivity but also the intensity of the pseudo-molecular ions, $[M+H]^+$ or $[M-H]^-$ signals. Hence, the mass spectra of the five standards recorded in ESI (+ and −) and APCI (+ and −) were compared. In general, the mass spectra obtained using ESI interface showed some corresponding fragmentation patterns as in APCI interface. By comparing the mass spectra acquired in positive mode, however, an obvious trend may be observed when ESI is used. A strong sodium adduct with the analyte signal, $[M+Na]^+$ was always observed in ESI interface, however, no sodium adduct was detected when the APCI source is used (Fig. 4). This finding was also supported by the previous literatures which reported that background concentration of sodium is almost always present in ESI samples but not in APCI samples [25,26]. One may think that quassinoids with the carbonyl functional group are readily donate a lone pair of electrons to form stable sodium adducts. Additionally, in the current investigation we have found that sodium adducts of analyte, $[M+Na]^+$, was often more abundant when flow injection analysis was performed in contrast with the injection of the standards through the chromatographic column (data not shown). Hence, the chromatography column will reduce the sodium adduct signals in ESI. Obviously, the occurrence of adduct does affect the abundance of the protonated molecule and subsequently lowering the detection limit of the analyte since the total analyte signal is divided over several *m/z* values.

In fact, innumerable studies have been carried out on electrospray ionization and have shown the predominance of sodium adduct, $[M+Na]^+$ and the lack of protonated molecular ion, $[M+H]^+$ [25,26]. The result of this study supported the previous finding. Out of five compounds, only two gave pseudo-molecular ion $[M+H]^+$, namely 13α(21)-epoxyeurycomanone (**2**) and 13,21-dihydroeurycomanone (**5**) (Fig. 4b(i) and e(i)). Aside from this, the MS spectrum of **1** which was acquired from the APCI positive mode (Fig. 4a(ii)) demonstrated high background noise when compared with that ESI positive mode (Fig. 4a(i)). Similarly, when the MS spectra of **3** and its glycoside **4** were recorded in the positive ion mode of APCI (Fig. 4c(ii) and d(ii), respectively), too many fragment ions were produced, showing that too many fragmentation pathways are opened. In fact, extensive fragmentation of a compound is particularly useful only in providing the structural information of the compound but not in MS/MS quantitative analysis. This is because MS spectra that exhibiting a complicated fragmentation pattern usually associated with significant reduction in the most abundant ion of that compound. Hence, it often hampers the selection of that ion to be quantified. It was also noteworthy that the interface with appropriate ionization mode which gave the low background ions in MS spectra gets preferential consideration.

In the present study, the quassinoids (except **4**, which losses the glucose unit together with two water molecules) showed a dominant fragmentation pathway involving the loss of H_2O. The quassinoids either exhibited neutral losses of 18 or 36 mass units, corresponding to the sequential losses of H_2O, $[M+H-H_2O]^+$ or $[M+H-2H_2O]^+$ from the precursor ion $[M+H]^+$. The fragmentation of the **1** in ESI + yielded a $[M+H-H_2O]^+$ base peak without any other fragmentation as depicted in Fig. 4a(i). The ESI + mass spectrum of **5** showed a signal at *m/z* 433 and 411, which analyzed for the pseudo-molecular ions, $[M+Na]^+$ and $[M+H]^+$, respectively, with other notable fragment ions at *m/z* 393, 375 and 357, due to the consecutive neutral losses of H_2O from the corresponding $[M+H]^+$ ion (Fig. 4e(i)). In ESI+, **3** produced a prominent ion at *m/z* 375, which can be attributed to loss of two water molecules from the protonated molecular ion $[M+H]^+$. In addition, characteristic ions also observed at *m/z* 357, 327, 299 and 281. Fragment ion at *m/z* 357 is due to the subsequent lost of a water molecule from that daughter ion with *m/z* 375. The *m/z* ion 357 then underwent the losses of $-CH_2O-$ fragment to generate an ion at *m/z* 327. The resulting fragment at *m/z* 327 underwent further CO neutral losses leading to fragment ion at *m/z* 299. Meanwhile, the presence of the fragment at *m/z* 281 for **3** suggested another neutral loss of H_2O from ion at *m/z* 299 (Fig. 4c(i)). The fragmentation behavior of **4** in ESI+ was very similar to that of **3** (Fig. 4d(i)). Compound **4** gave the most dominant fragment with *m/z* 375 due to the cleavage of sugar moiety and the loss of two water molecules. Consequently, the *m/z* 375 ion lost another water molecule to give ion at *m/z* 357. The presence of the fragment at *m/z* 299 in the MS spectrum, originating from the consecutive cleavage of a $-CH_2O-$ residue followed by the neutral loss of CO from product ion at *m/z* 357, indicated the glycoside exhibited the same types of small neutral losses as describe for the aglycone. The fragmentation behavior of **2** was very different from other quassinoids. In its full scan MS spectrum (Fig. 4b(i)), the prominent signal was not $[M+H-H_2O]^+$ at *m/z* 407 but the $[M+H-CO-H_2]^+$ ion at *m/z* 395.

One important observation, based on study of the five quassinoids, was that the $[M-H]^-$ ions showed up in all ESI mass spectra. This may be useful in determining the molecular mass of quassinoid using ESI negative mode because the quassinoids of interest readily gave pseudo-molecular ion, $[M-H]^-$ signals, however, not all quassinoids able to yield pseudo-molecular ion, $[M+H]^+$ signals when positive mode was applied. Furthermore, $[M-H-H_2O]^-$ fragments formed due to the loss of one water molecule from the pseudo-molecular ion $[M-H]^-$ were also observed. As a result, the ionization mechanism of quassinoids in negative ion mode of ESI

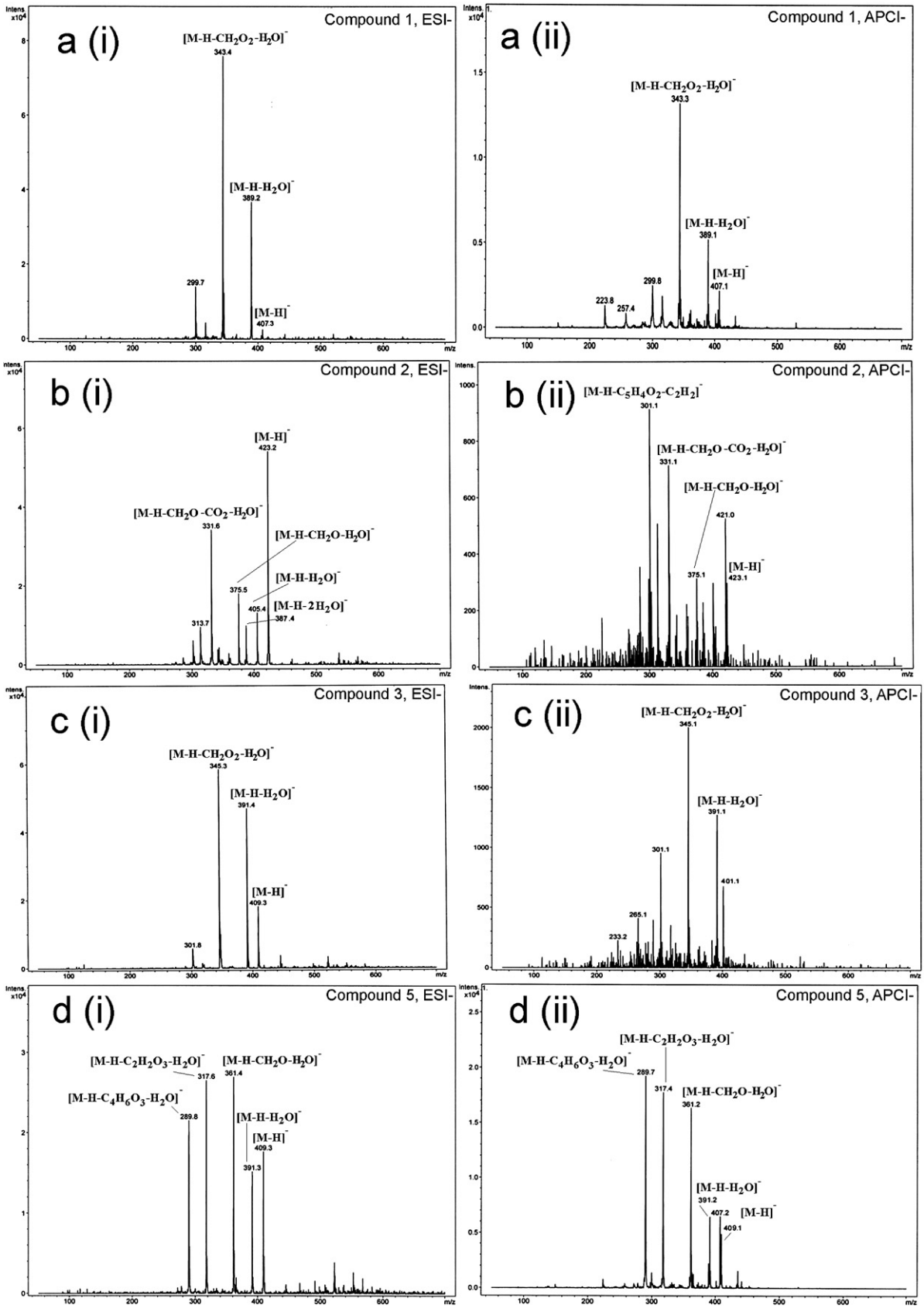

Fig. 5. Negative mode (i) ESI-MS and (ii) APCI-MS spectra of (a) eurycomanone (**1**), (b) 13α(21)-epoxyeurycomanone (**2**), (c) eurycomanol (**3**), (d) 13,21-dihydroeurycomanone (**5**), and (e) eurycomanol-2-*O*-β-D-glucopyranoside (**4**) using FIA.

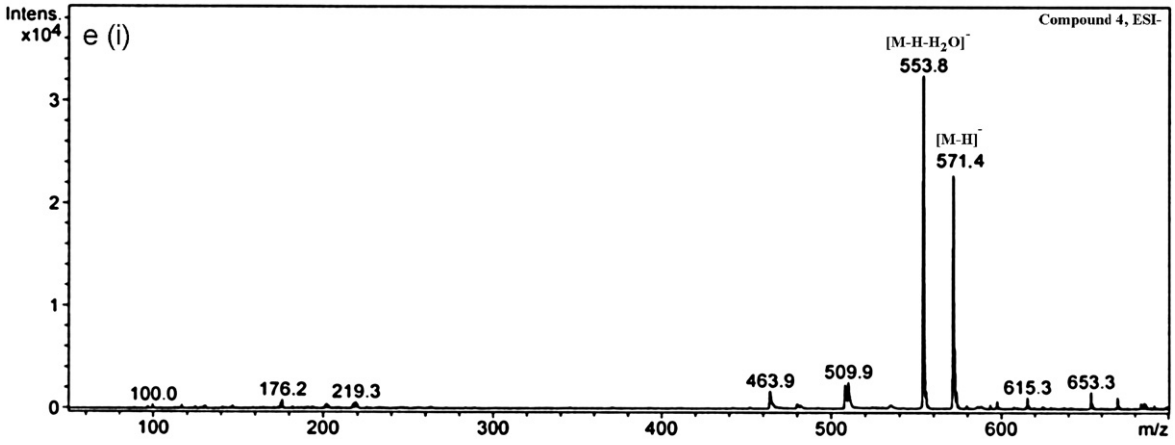

Fig. 5. (*Continued.*)

was concluded to proceed through the formation of deprotonated molecular ions $[M-H]^-$. As seen in ESI-MS, the pseudo-molecular ions $[M-H]^-$ of **2**, **3** and **4** did not show extensive fragmentation, while in APCI mode, these ions became somewhat less stable and more prone to fragmentation (Fig. 5b(ii) and c(ii)). Hence, APCI negative ion mode is not suitable for the analysis of these compounds. The ESI- and APCI-mass spectra of **1** showed a pseudo-molecular ion $[M-H]^-$ at *m/z* 407 and its fragmentation led to one fragment at *m/z* 389 corresponding to the neutral loss of a water molecule. The fragment ion at *m/z* 343 (base peak) was generated from successive losses of $-CH_2O_2-$ moiety and a water molecule from $[M-H]^-$ ion. The mass spectra of **5** showed a quassi-molecular ion $[M-H]^-$ at *m/z* 409. Other significant fragment ions at *m/z* 391$[M-H-H_2O]^-$, 361 $[M-H-CH_2O-H_2O]^-$, 317 $[M-H-C_2H_2O_3-H_2O]^-$ and 289 $[M-H-C_4H_6O_3-H_2O]^-$ were observed. Meanwhile, the fragmentation patterns of **2** showed close resemblance to that of **5**. In addition to $[M-H]^-$, $[M-H-H_2O]^-$ and $[M-H-CH_2O-H_2O]^-$ fragment ions at *m/z* 423, 405 and 375, respectively, fragmentation of **2** also produced neutral loss of 36 mass units subsequent to the loss of two water molecules, $[M-H-2H_2O]^-$ from the precursor ion $[M-H]^-$. Similarly, the fragment ions of $[M-H-H_2O]^-$ and $[M-H-CH_2O_2-H_2O]^-$ from **3**, observed at *m/z* 391 and 345, respectively, demonstrated identical core structures of to those of **1**.

3.2.6. Effect of capillary voltage, nebulizing pressure, drying gas flow rate and drying gas temperature

The effect of capillary voltage represents a critical parameter in ESI-MS and has been intensely studied [21]. This is because the electrical field is required to generate fine charged droplets by which a stable ion signal can be generated. Thus, the capillary voltage was tested between 2.5 and 4.5 kV. In general, the MS signals of the quassinoids showed an increase with increasing capillary voltage (Fig. 6(a)). **3** and **4** gave the highest TIC response at capillary voltage of 4.5 kV while **1** and **2** at capillary voltage of 3.5 kV. Hence, the optimum value for this parameter was found at 4.5 kV. The drying gas flow rate was varied between 6 and 12 L min^{-1}. In general, the intensity of the MS signal showed a slight increment and reached a maximum (between 8 and 10 L min^{-1}) by increasing the drying gas flow rate; further increase of flow (above 10 L min^{-1}) resulted in decrement of the signal response, as showed in Fig. 6(b) Hence, a compromise between the five analytes was reached with a flow rate of 8 L min^{-1} in positive ESI. The dry gas temperature of ESI positive was tested between 250 °C and 350 °C. It was found that the response of the analytes increased when this parameter was increased (Fig. 6(c). Although **2** and **3** showed a downturn trend at drying gas temperature 340 °C, the optimal value were set at 350 °C, a compromise between the MS response of the five standards. The nebulizing pressure not only plays a vital role in the generation of an electrically charged aerosol but also to obtain a stable spray in ESI interface [27]. Thus, in the present study, the nebulizing pressure was varied from 30 to 60 psi. As depicted in Fig. 6(d), the intensity of MS signal showed a slight improvement at 35 psi followed by decreased of response with increasing the nebulizing pressure. As a result, the optimal nebulizing pressure for positive ESI was set at 35 psi.

3.2.7. Effect of capillary exit offset voltage

The capillary exit offset played a major role in the fragmentation and the cleavage processes of the molecules. By carefully adjusting the capillary exit offset voltage of the transfer capillary of the API interface manually, fragmentation could be suppressed or enhanced offering the possibility to increase the sensitivity of the analytes. Supplementary material 4 shows that ion signal at *m/z* 391 ($[M+H-H_2O]^+$) produced by **1** appeared as base peak at low capillary exit offset voltage (10–80 V). However, the signal of $[M+Na]^+$ at *m/z* 431 became more predominant when high capillary exit offset voltage were employed (110–210 V). As indicated in Fig. 7, the optimum capillary exit offset voltage for $[M+H-H_2O]^+$ ion was 80 V. At capillary exit offset voltage between 10 and 110 V, **2** showed a pseudo-molecular ion $[M+H]^+$ and sodiated ion $[M+Na]^+$ at *m/z* 425 and 447, respectively, with a characteristic fragment ion $[M+H-H_2O]^+$ at *m/z* 407. When the capillary exit offset voltage was further increased (160–210 V), intensive fragmentation caused the loss of the $[M+H]^+$ signal (Supplementary material 5). Since $[M+H]^+$ ion of **2** gave the highest response at 60 V as shown in Fig. 7, this value was chosen for subsequent quantification.

At low capillary exit offset voltage (10 V), the mass spectrum of **3** consisted of several characteristic fragment ions at *m/z* 327 and 375 which were identified as $[M+H-3H_2O-CH_2O]^+$ and $[M+H-2H_2O]^+$, respectively. In addition, the sodium adduct ions of **3** could be observed at *m/z* 433. Further increased of the capillary exit offset voltage (up to 210 V) leading to more intense fragmentation and hence, reduced its signal intensity. As showed in Supplementary material 6 and Fig. 7, the highest intensity of the fragment ion ($[M+H-2H_2O]^+$) observed when 60 V of capillary exit offset voltage was applied. Beyond this voltage, the intensity of this ion decreased significantly. As a result, the optimum capillary exit offset voltage to analyze the $[M+H-2H_2O]^+$ ion of **3** was 60 V. Increasing the capillary exit offset voltage from 10 to 210 V gave a tremendous increasing response of sodium adduct ion $[M+Na]^+$ of **4** (Supplementary material 7). In fact, this ion was the base peak in the MS spectra when higher capillary exit offset voltage was employed (160–240 V). Major fragmentation was also observed

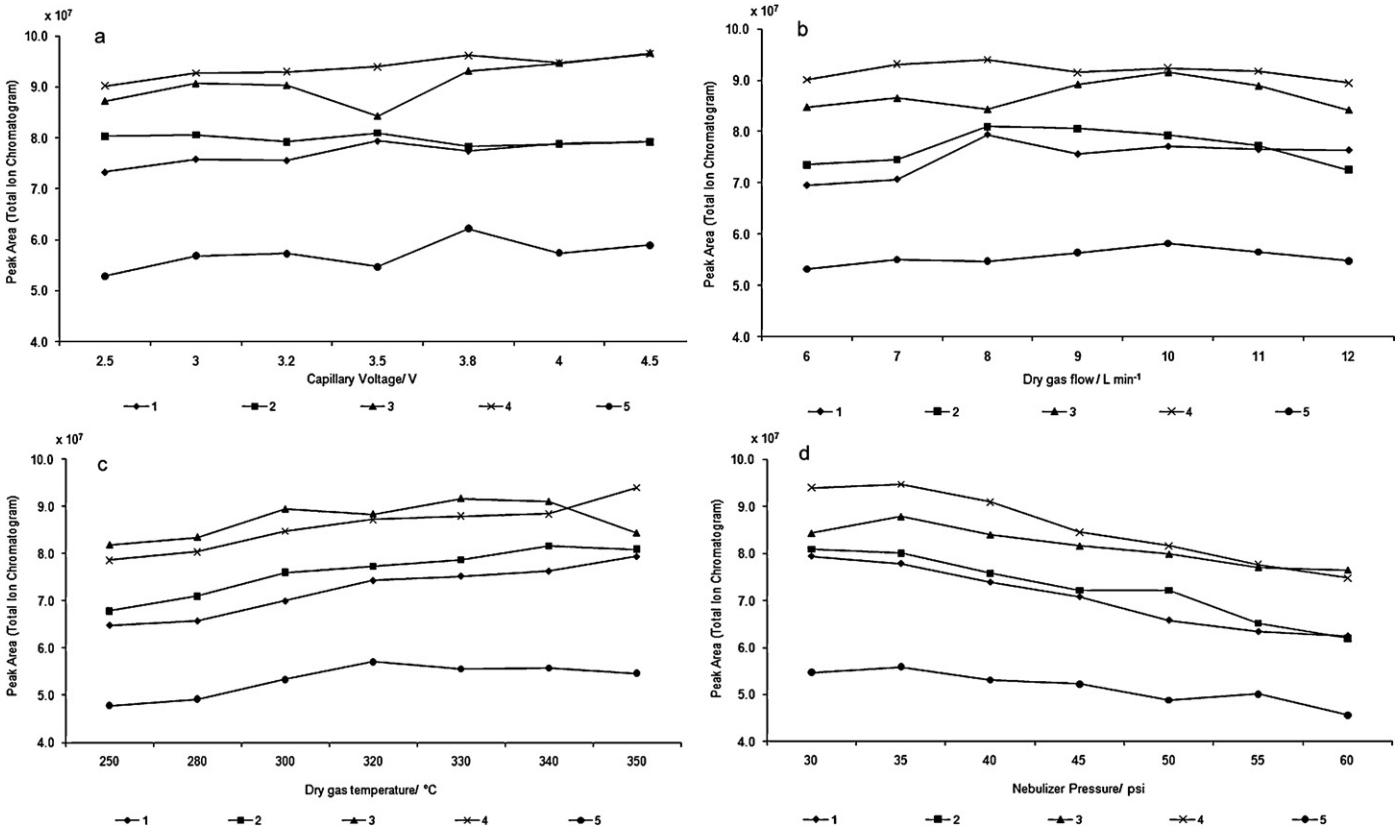

Fig. 6. Influence of (a) capillary voltage, (b) dry gas flow, (c) dry gas temperature, and (d) nebulizer pressure on MS response of the major quassinoids in positive ESI. Compound identification: eurycomanone (**1**), 13α(21)-epoxyeuryromanone (**2**), eurycomanol (**3**), eurycomanol-2-O-β-D-glucopyranoside (**4**) and 13,21-dihydroeurycomanone (**5**).

under these conditions. As showed in Fig. 7, the intensity of the fragment ion $[M+H-C_6H_{12}O_6-2H_2O]^+$ of **4** increase steadily to a maximum around 60 V, then decrease continuously to a minimum around 160 V and showed a slightly upturn in intensity at 210 V. Based on these data, a capillary exit offset voltage of 60 V was used to monitor the $[M+H-C_6H_{12}O_6-2H_2O]^+$ fragment ion of **4**.

The extent of fragmentation of **5** was considered high even at low capillary exit offset voltage of 10 V. From Supplementary material 8, **5** not only gave the pseudo-molecular ion $[M+H]^+$ and the sodium adduct $[M+Na]^+$ peaks at *m/z* 411 and 433, respectively, but also other major fragments at *m/z* 261 $[M+H-C_5H_8O_4-H_2O]^+$ and 393 $[M+H-H_2O]^+$. Increasing the capillary exit offset voltage from 10 to 110 V significantly depresses the $[M+H]^+$ signal. It was apparent that as more of the $[M+H]^+$ ion being fragmented through the loss of a water molecules at low voltage (10–80 V), the signal intensity of $[M+H-H_2O]^+$ ion at *m/z* 393 increased. However, voltage up to 160 V increased fragmentation and under these conditions many fragment ions appeared but none of them is predominant. Fig. 7 indicated that **5** gave the highest response of $[M+H]^+$ ion at capillary exit offset voltage of 60 V. Hence, this value was chosen to monitor the protonated molecule of **5**.

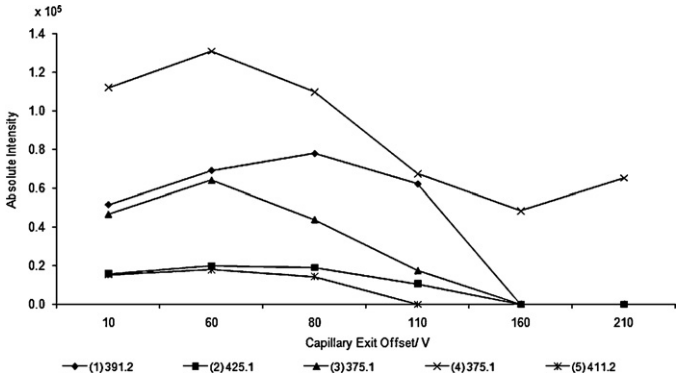

Fig. 7. Effect of the capillary exit offset voltage on signal intensity of $[M+H-H_2O]^+$ ion of eurycomanone (**1**); $[M+H]^+$ ion of 13α (21)-epoxyeurycomanone (**2**); 13,21-dihydroeurycomanone (**5**), respectively; $[M+H-2H_2O]^+$ ion of eurycomanol (**3**), and $[M+H-C_6H_{12}O_6-2H_2O]^+$ ion of eurycomanol-2-*O*-β-D-glucopyranoside (**4**).

3.2.8. *Effect of fragmentation amplitude*

Collision-induced dissociation of the isolated precursor ion took place when the fragmentation amplitude was applied on that ion. This resulted in product ion(s) that can be used for MS/MS quantification. However, extensive MS/MS fragmentation of the precursor ion is usually less favorable, because the presence of abundant product ions may effectively dilute the ion signal and thus, reducing the sensitivity in MS/MS mode. The protonated molecular ion $[M+H]^+$ was chosen as precursor ion for MS/MS fragmentation analysis of 13α(21)-epoxyeurycomanone (**2**) and 13,21-dihydroeurycomanone (**5**), respectively. On the other hand, $[M+H-H_2O]^+$, $[M+H-2H_2O]^+$ and $[M+H-C_6H_{12}O_6-2H_2O]^+$ ions, exhibiting the highest intensity signal at full scan of the mass spectra were selected as the precursor ions for MS/MS fragmentation analysis of eurycomanone (**1**), eurycomanol (**3**) and eurycomanol-2-*O*-β-D-glucopyranoside (**4**), respectively. Supplementary material 9 showed the MS/MS fragmentation pattern of the aforementioned precursor ion of the five standards. As can be seen, the fragmentation pattern of precursor ion of quassinoids, except 13α(21)-epoxyeurycomanone (**2**) and 13,21-dihydroeurycomanone (**5**), were complex and a number of products ions were produced. Indeed, precursor ion of eurycomanol (**3**), $[M+H-2H_2O]^+$ (*m/z* 375), displayed the same MS/MS fragmenta-

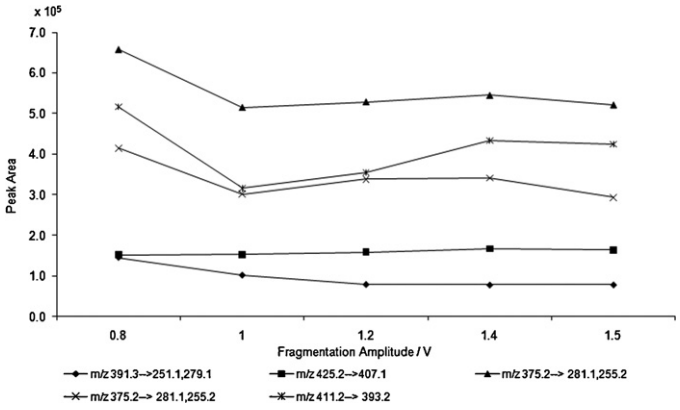

Fig. 8. Influence of fragmentation amplitude voltage on the MRM peak area of $[M+H-H_2O]^+$ ion of eurycomanone (**1**); $[M+H]^+$ ion of 13α(21)-epoxyeurycomanone (**2**) and 13,21-dihydroeurycomanone (**5**), respectively; $[M+H-2H_2O]^+$ ion of eurycomanol (**3**), and $[M+H-C_6H_{12}O_6-2H_2O]^+$ ion of eurycomanol-2-*O*-β-D-glucopyranoside (**4**) in positive ESI.

tion pathways as compared to those of $[M+H-C_6H_{12}O_6-2H_2O]^+$ (*m/z* 375) ion of eurycomanol-2-*O*-β-D-glucopyranoside (**4**), indicating that the major fragments at *m/z* 357, 327, 299, 281 and 255 were identical to those in **4**. Further assignments of these ions can be made as follows: *m/z* 357 (375-H_2O), *m/z* 327 (375-H_2O–CH_2O), *m/z* 299 (375-H_2O–CH_2O–CO), *m/z* 281 (375-2H_2O–CH_2O–CO), *m/z* 255 (375-2H_2O–CH_2O–2CO+2H). In addition to the loss of 30 mass units (corresponded to the cleavage of the epoxy group, CH_2O), the MS/MS fragmentation pathway of **3** and **4** was also notable for the neutral loss of CO. This type of cleavage may lead to the contraction of the quassinoid's ring in **3** and **4**. Eurycomanone (**1**) which also could not produce a stable protonated molecular ion of $[M+H]^+$ demonstrated an extensive MS/MS fragmentation on the precursor ion of $[M+H-H_2O]^+$ at *m/z* 391. The product ion spectrum obtained, which is shown in Supplementary material 9, indicated that there was no predominant fragment ion generated, but only certain fragmentation patterns emerge. Obviously, the fragmentation pathway was characterized by the loss of H_2O (*m/z* 373), loss of CO followed by the loss of H_2O (*m/z* 345), loss of CO followed by the double loss of H_2O (*m/z* 327) and loss of CO followed by the triple loss of H_2O (*m/z* 309) from the precursor ion at *m/z* 391. In addition, the two significant fragments at *m/z* 279 and 251 were assigned to $[M+H-4H_2O-CO-CH_2O]^+$ and $[M+H-4H_2O-2CO-CH_2O]^+$ daughter ions, respectively. Both **2** and **5**, which could produce the stable pseudo-molecular ion $[M+H]^+$, readily gave the product ion at *m/z* 393 and 407, respectively. These ions were attributed to the neutral loss of a H_2O molecule from their respective precursor ion, $[M+H]^+$. As shown in Supplementary material 9, fragment ions at *m/z* 393 and 407 were observed as the primary signal of **2** and **5**, respectively, in the product ion scan. Other product ions only existed in relatively low abundance. From the MS/MS fragmentation, the product ion profile and the predominant product ion for each of the analyte could be determined.

By optimizing the fragmentation amplitude voltages, however, the abundance of a specific product ion can further be improved. This was achieved by monitoring the decay of the particular precursor ion over a range of fragmentation amplitudes voltages, via from 0.8 to 1.5 V. Compound **2** and **5** showed the persistence of the most prominent peak at *m/z* 407 and 393, respectively, in the product ion spectra when the fragmentation amplitudes were varied between 0.8 and 1.5 V. This suggested that the MRM transitions *m/z* 425/407 and *m/z* 411/393 could be used for the detection of **2** and **5**, respectively, in the MS/MS analysis. As depicted in Fig. 8, fragmentation amplitude of 0.8 V gave the highest MRM response of **2** and **5**. Therefore, the MRM transitions *m/z* 425/407 and *m/z* 411/393 at fragmentation amplitude of 0.8 V was chosen for the quantification of **2** and **5**, respectively. Owing to **3** and **4** could not produce a predominant product ion when the fragmentation amplitudes was varied between 0.8 and 1.5 V, the sum of the peak areas of the two highest product ions from multiple reaction monitoring (MRM) mode were used. Both **3** and **4** could produce the precursor ion at *m/z* 375 in ion source, and fragments at *m/z* 281 and 255 were the product ions of *m/z* 375. Thus, the peaks of **3** and **4** could be detected when scanning with transition *m/z* 375/281, 255. As showed in Fig. 8, the precursor/product ion pair of *m/z* 375/281, 255 for **3** and **4** was the most responsive at low fragmentation amplitude voltage. Consequently, the fragmentation amplitude voltage of 0.8 V was selected for the transition *m/z* 375/281, 255. When the fragmentation amplitudes was varied between 0.8 and 1.5 V, the precursor ion of **1**, $[M+H-H_2O]^+$ produced a number of product ions. The two highest product ions at *m/z* 279 and 251 were identified. As a result, the transition *m/z* 391/279, 251 was selected monitor **1** in MRM mode. Again, the fragmentation amplitudes of 0.8 V gave maximum response of **1**, as can be seen in Fig. 8 and thus was chosen for the quantitative determination of **1** in MRM mode.

3.3. Method validation

3.3.1. Linear ranges, limit of detections (LODs) and limits of quantifications (LOQs), precisions, accuracies and recoveries

ESI-MS has a relatively narrow linear dynamic range. Besides that, this linear dynamic range is a compound-dependent parameter. According to Law and Temesi [28], at best it is possible to achieve 3–4 orders of magnitude when ESI-MS operated at low concentration using an optimized compound specific method, while Hakala et al. [29] reported the linear quantitative range of ESI was only 2–3 orders of magnitude. According to Cech et al. [30], the deviations from linearity occur at high concentrations (usually around 10^{-5} M) as ESI response becomes saturated, and at low concentrations due to background interference.

In the present study, it was found that the calibration curves for all the chemical standards of *E. longifolia* also displayed a narrow linearity range as shown in Table 2. At concentration above 30.0 $\mu g\,mL^{-1}$, the calibration curves exhibit non-linear behavior. It was noted that the report by Pohlit et al. [10] also showed the comparable linearity ranges of 0.25–5.0 $\mu g\,mL^{-1}$ and 0.5–10.0 $\mu g\,mL^{-1}$ when using the LC–ESI-MS for the determination of quassinoids. The calibration curves for **3**, **5** and **2** were linear over the concentration range of 0.5–30.0 $\mu g\,mL^{-1}$ (r^2 = 0.9998, 0.9999 and 0.9994, respectively), for **4** was 1.0–30.0 $\mu g\,mL^{-1}$ (r^2 = 0.9961) whereas, for **1** was 0.5–20.0 $\mu g\,mL^{-1}$ (r^2 = 0.9969). The LOD values of compounds **1**, **2**, **5**, **3**, and **4** were 0.08, 0.05, 0.03, 0.1 and 0.1 $\mu g\,mL^{-1}$, respectively, measured by LC–ESI-MS analysis using isolation mode (single ion monitoring, SIM) at a S/N ratio of 3 (Table 2). The LOQ value of compounds **1**, **2**, **5** and **3** was 0.5 $\mu g\,mL^{-1}$ and for compounds **4** was 1.0 $\mu g\,mL^{-1}$ (Table 2). The intra-day and inter-day precisions and accuracies for *E. longifolia* are shown in Table 3. The accuracy values of quassinoids were between 97.24 and 105.20%, while the corresponding precision values expressed as % RSD were between 0.38 and 5.72% for both intra-day and inter-day analysis, indicating that the method was reliable and repeatable. The recovery for the measurements of the quassinoid was shown in Table 4. The present method produced a satisfactory quassinoids recovery of 88.37–118.18%.

3.3.2. Application of the validated LC–ESI-MS method for the simultaneous analysis of major quassinoids in bioactive extract of *E. longifolia*

Quantification in LC–MS-MS methods is usually based on the ratio of base peak ion (the specific product ion of the analyte) to the base peak ion of the internal standard [31]. Although the use of

Table 2
Regression equations, correlation coefficients r^2, linearity ranges and limits of detection (LOD) and quantification (LOQ) for the 5 chemical standards of *Eurycoma longifolia*.

Compound[a]	Regression equation	Linear range (μg mL^{-1})	r^2	LOD[b] (μg mL^{-1})	LOQ[b] (μg mL^{-1})
1	$y = 786{,}404x + 224{,}363$	0.5–20.0	0.9969	0.08	0.5
2	$y = 54{,}718x - 21{,}965$	0.5–30.0	0.9994	0.05	0.5
3	$y = 674{,}639x - 126{,}401$	0.5–30.0	0.9998	0.1	0.5
4	$y = 388{,}490x - 77{,}695$	1.0–30.0	0.9961	0.1	1.0
5	$y = 293{,}625x - 71{,}466$	0.5–30.0	0.9999	0.03	0.5

[a] Compound identification: eurycomanone (**1**), 13α(21)-epoxyeuryromanone (**2**), eurycomanol (**3**), eurycomanol-2-O-β-D-glucopyranoside (**4**) and 13,21-dihydroeurycomanone (**5**).
[b] 5 μL injected.

Table 3
Intra-day and inter-day precision and accuracy values of *Eurycoma longifolia* analyzed by LC–ESI-MS detection method.

Concentration (μg mL^{-1})	Intra-day ($n = 5$)		Inter-day ($n = 5$)	
	Accuracy (% true value)	Precision (RSD, %)	Accuracy (% true value)	Precision (RSD, %)
Eurycomanone (**1**)				
0.50	101.55	3.34	97.24	4.13
1.00	101.80	1.50	100.66	3.90
5.00	101.46	1.00	100.14	1.45
10.00	99.98	1.39	99.42	1.58
20.00	102.11	0.75	100.18	0.41
13α (21)-Epoxyeuryromanone (**2**)				
0.50	105.20	5.52	98.74	4.82
5.00	100.53	0.83	100.92	0.83
10.00	99.54	1.41	100.72	0.75
25.00	100.18	1.62	100.20	0.55
30.00	99.83	0.38	99.71	0.95
Eurycomanol (**3**)				
0.50	99.76	5.22	99.84	4.66
5.00	98.88	1.99	100.06	1.26
10.00	99.13	1.82	101.00	1.11
25.00	99.73	3.01	99.72	0.56
30.00	99.37	2.54	100.36	1.00
Eurycomanol-2-O-β-D-glucopyranoside (**4**)				
1.00	102.17	2.93	103.30	4.40
5.00	97.24	2.05	99.11	1.77
10.00	104.45	1.75	102.53	1.74
20.00	101.34	2.10	99.61	1.28
30.00	101.67	2.02	99.64	0.57
13,21-Dihydroeurycomanone (**5**)				
0.50	103.79	5.72	99.62	3.80
5.00	101.33	1.32	99.97	0.80
10.00	99.23	2.35	99.80	1.00
25.00	100.24	1.72	100.08	0.59
30.00	99.50	1.20	100.13	0.41

Table 4
Recovery values ($n = 4$) of spiked quassinoids in *Eurycoma longifolia* bioactive extract.

Quassinoids[a]	Spiked concentration (μg mL^{-1})	Mean measured concentration (μg mL^{-1})	Recovery ($n = 4$)	
			Mean (%)	Precision (RSD, %)
1	0.50	0.49	97.24	9.29
	5.00	4.42	88.37	0.79
	20.00	20.80	103.98	5.95
2	0.50	0.52	103.07	3.69
	5.00	4.73	94.65	9.55
	20.00	20.22	101.12	6.81
3	0.50	0.49	98.49	4.48
	5.00	5.19	103.75	5.66
	20.00	21.92	109.60	6.47
4	0.50	0.52	104.88	4.69
	5.00	5.64	112.73	7.42
	20.00	23.64	118.18	4.23
5	0.50	0.47	93.61	3.53
	5.00	4.77	95.39	9.04
	20.00	18.72	93.59	5.66

[a] Compound identification: eurycomanone (**1**), 13α(21)-epoxyeuryromanone (**2**), eurycomanol (**3**), eurycomanol-2-O-β-D-glucopyranoside (**4**) and 13,21-dihydroeurycomanone (**5**).

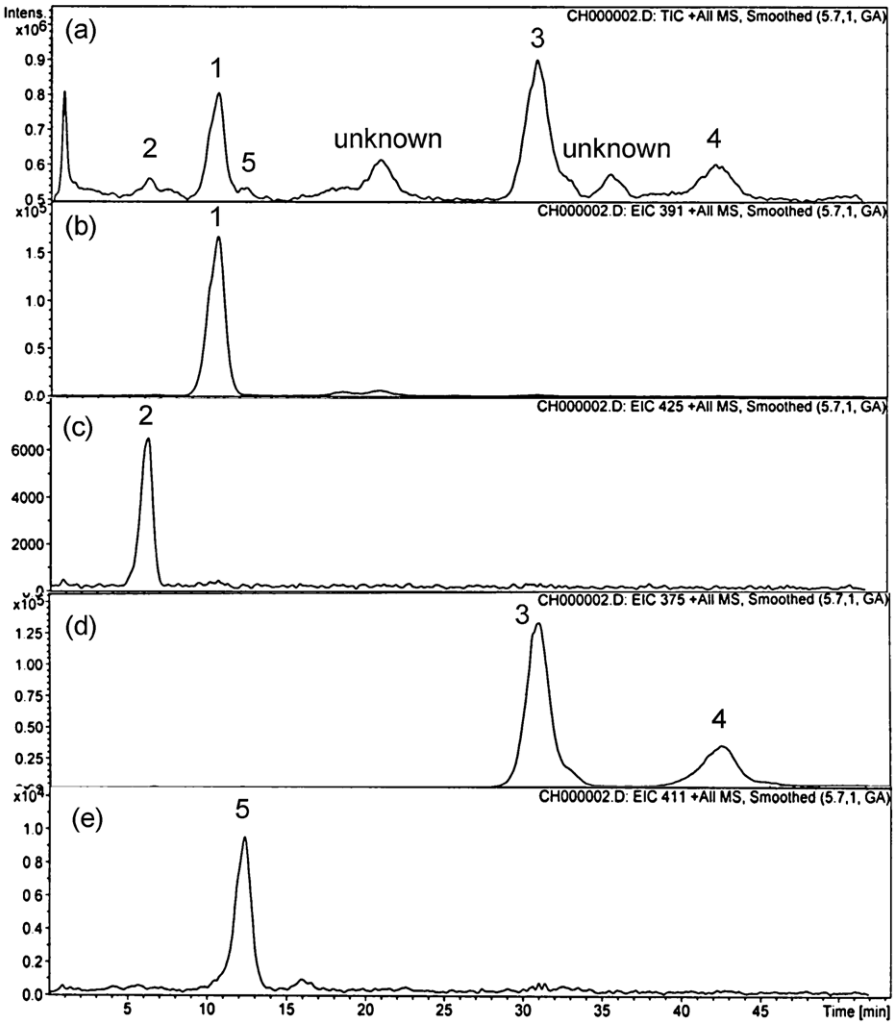

Fig. 9. (a) LC–TIC chromatogram of the bioactive fraction in positive ESI. EIC chromatogram of (b) eurycomanone (**1**), (c) 13α (21)-epoxyeuryromanone (**2**), (d) eurycomanol (**3**), (d) eurycomanol-2-O-β-D-glucopyranoside (**4**), and (e) 13,21-dihydroeurycomanone (**5**).

an internal standard is always recommended for a more accurate quantitative analysis, Ding et al. [32] reported that under certain circumstances it may not cause any improvement in the result. In fact, there are several criteria to be considered in the selection for an ideal internal standard. An internal standard should be structurally analogue to the target compound and do not exhibit noticeable matrix effect, responded well in ESI (+) mode, and also, eluted within the same chromatographic time frame as the analyte. Owing to the difficulties in obtaining an appropriate compound as an internal standard, the quantitative analysis was conducted without internal standard and was based on external standard calibration method.

The LC–ESI-MS detection method was applied to study the various batches of Tongkat Ali containing the quassinoids in the 30% methanol fraction eluted from resin chromatography of methanol extract of the root of *E. longifolia* obtained from various places. The result of this study for a representative batch is shown in Fig. 9. Table 5 summarizes the quassinoids content of the bioactive fraction 2 from different batches. The relative distribution of the quassinoids showed that batches 2, 4, and 5 have the highest content of eurycomanol (**3**), while in batches of 3 and 6, eurycomanol-2-O-β-D-glucopyranoside (**4**) was the highest. Except in batch 1, the relative distributions of eurycomanol-2-O-β-D-glucopyranoside (**4**) were relatively higher than that of eurycomanone (**3**). In general, the relative distribution of 13α(21)-epoxyeuryromanone (**2**) and 13,21-dihydroeurycomanone (**5**) in different batches were comparable, except in batches 1 and 3 which showed a significantly lower relative distribution of 13,21-dihydroeurycomanone (**5**), at 0.08 and 0.07, respectively.

As indicated in Table 5, eurycomanone (**1**), eurycomanol (**3**) and eurycomanol-2-O-β-D-glucopyranoside (**9**) were the main quassinoids in the bioactive extracts, whereas 13α(21)-epoxyeuryromanone (**2**) and 13,21-dihydroeurycomanone (**5**) were present in much lower quantity. The observed high degree of variability in the quassinoids content in this study could be due to environmental factors such as harvesting time, growing conditions or altitude.

The concentration range of five quassinoids that present in the bioactive fractions from different batches was summarized in Table 6. One of the test batches (batch 3) has been compared with artemisinin for antimalarial activity by Wernsdorfer et al. [16] and exhibited potent antimalarial activity (IC_{50} of 3.4-fold less potency than that of artemisinin). In our present study, the quassinoids in batch 3 was found to be in the following ranges: 7.16–7.34% for eurycomanone (**1**), 1.44–1.75% for 13α(21)-epoxyeuryromanone (**2**), 5.00–5.31% for eurycomanol (**3**), 9.08–9.70% for eurycomanol-2-O-β-D-glucopyranoside (**4**) and 0.45–0.51% for 13,21-dihydroeurycomanone (**5**). Hence, for good antimalarial activity against chloroquine-resistant *P. falciparum*,

Table 5
Content of quassinoids in 30% methanol fraction eluted from resin chromatography of methanol extract of the root of *E. longifolia* purchased by Hovid and Biotropic Berhad from various sources, locations and harvesting times.

Batch	Content of major quassinoids (% ±SEM of sample, $n = 4$)					Relative distribution of quassinoids				
	1	**2**	**3**	**4**	**5**	**1**	**2**	**3**	**4**	**5**
1	9.95 ± 0.10	3.90 ± 0.03	9.06 ± 0.06	7.59 ± 0.06	0.78 ± 0.01	1	0.39	0.91	0.76	0.08
2	8.08 ± 0.04	1.26 ± 0.02	17.24 ± 0.10	10.95 ± 0.09	1.55 ± 0.02	1	0.16	2.13	1.35	0.19
3	7.25 ± 0.02	1.64 ± 0.04	5.21 ± 0.04	9.39 ± 0.07	0.47 ± 0.01	1	0.23	0.72	1.30	0.07
4	5.65 ± 0.04	0.78 ± 0.004	15.32 ± 0.10	14.52 ± 0.10	1.22 ± 0.01	1	0.14	2.71	2.57	0.22
5	8.23 ± 0.01	1.43 ± 0.02	19.75 ± 0.07	11.25 ± 0.08	1.76 ± 0.01	1	0.17	2.40	1.37	0.21
6	6.73 ± 0.07	1.72 ± 0.08	13.63 ± 0.23	19.95 ± 0.45	1.04 ± 0.03	1	0.26	2.02	2.96	0.15

Table 6
The concentration range of five quassinoids from the six batches of bioactive fractions.

Quassinoid	Concentration range (%) of six batches studied	Concentration range (%) of batch 3[a]
Eurycomanone (**1**)	5.65–9.95	7.16–7.34
13α (21)-Epoxyeuryromanone (**2**)	0.78–3.90	1.44–1.75
Eurycomanol (**3**)	5.21–19.75	5.00–5.31
Eurycomanol-2-O-β-D-glucopyranoside (**4**)	7.59–19.95	9.08–9.70
13,21-Dihydroeurycomanone (**5**)	0.47–1.76	0.45–0.51

[a] Antimalarial activity was studied by Wernsdorfer et al. [16] on batch 3.

the bioactive extract should contain the quassinoids within the described range.

4. Conclusions

Electrospray ionization (ESI) and atmospheric-pressure chemical ionization (APCI) techniques, in both positive and negative ion modes, were compared for the optimized determination of eurycomanone (**1**), 13α(21)-epoxyeurycomanone (**2**), eurycomanol (**3**), eurycomanol-2-*O*-β-D-glucopyranoside (**4**) and 13,21-dihydroeurycomanone (**5**) by LC–MS. Of ESI and APCI, positive ion ESI provided the highest response for the test compounds. The used of methanol–water (9:91, v/v) as mobile phase was preferred rather than acetonitrile–water (4:96, v/v), due mainly to higher total ion chromatogram (TIC)-MS responses produced. The results of the present study also showed that the type of acidic modifier as well as its concentration had a great effect on the ionization efficiency of analytes. As a result, optimal ionization conditions for the aforementioned compounds were achieved in positive ion mode of ESI with an eluent system consisting of methanol and 0.1% of acetic acid. In addition, it was found that the nebulizer pressure, dry gas flow, dry gas temperature and capillary voltage which set at 35 psi, 8 L min^{-1}, 350 °C, and 4500 V, respectively, provided the best conditions for detection of these compounds in ESI positive ion mode. Studies on the fragmentation patterns of analytes in ESI positive ion mode indicated that only 13((21)-epoxyeurycomanone (**2**) and 13,21-dihydroeurycomanone (**5**) gave the pseudo-molecular ion $[M+H]^+$. Except for eurycomanol-2-*O*-β-D-glucopyranoside (**4**), all the quassinoids in the present studied showed a dominant fragmentation pathway involving the loss of H_2O from the precursor ion $[M+H]^+$. It was found that the Multiple Reaction Monitoring (MRM) mode for quantitative LC–ESI-MS was not suitable to analyze eurycomanone (**1**), eurycomanol (**3**) and eurycomanol-2-*O*-β-D-glucopyranoside (**4**) as these quassinoids could not produce a major fragment ion in the product ion spectra. Hence, selected ion monitoring (SIM) mode was employed to quantify the major precursor ions produced from these quassinoids. Subsequently, a new analytical LC–ESI-MS method was established. This newly developed method was validated and found to be accurate and precised. It was worthy noted that the use of this method has a great advantage to quantify the non-chromophoric quassinoids, named eurycomanol (**3**) and eurycomanol-2-*O*-β-D-glucopyranoside (**4**). This method was also applied for simultaneous determination of the major and minor quassinoids found in the various batches of bioactive extracts of *E. longifolia* developed for antimalarial treatment. The quantitative analysis with the optimized LC–MS method demonstrated that the various batches of *E. longifolia* bioactive extract did not fall within a narrow range of each chemical constituent. These batches which varied in range of each constituents concentration may be due to the age of the harvesting plant, the soil and environment conditions or grown at different altitudes. This method may be of value for routine quality assurance and can be used for the standardization of the bioactive quassinoids from the raw material or extract for antimalarial purpose.

Acknowledgements

The authors would like to thank Universiti Sains Malaysia for a Research University Golden Goose Grant No. 1001/PFARMASI/813006. Our special thanks also to Mr. Peter Sprenger from Bruker Biospin, Bangkok, Thailand for running NMR of the five quassinoids.

Appendix A. Supplementary data

Supplementary data associated with this article can be found, in the online version, at doi:10.1016/j.chroma.2011.02.014.

References

[1] M. Rauh, M. Groeschl, W. Rascher, Clin. Chem. 53 (2007) 902.
[2] E. Tareke, J.F. Bowyer, D.R. Doerge, Rapid Commun. Mass Spectrom. 21 (2007) 3898.
[3] N. Fabre, I. Rustan, E. de Hoffmann, J. Quetin-Leclercq, J. Am. Soc. Mass Spectrom. 12 (2001) 707.
[4] M. Biesaga, K. Pyrzynska, J. Chromatogr. A 1216 (2009) 6620.
[5] B. Canabate-Diaz, A. Segura Carretero, A. Fernandez-Gutierrez, A. Belmonte Vega, A. Garrido Frenich, J.L. Martinez Vidal, J. Duran Martos, Food Chem. 102 (2007) 593.
[6] E. de Rijke, H. Zappey, F. Ariese, C. Gooijer, U.A.T. Brinkman, J. Chromatogr. A 984 (2003) 45.
[7] M. Okano, N. Fukamiya, K.H. Lee, Stud. Nat. Prod. Chem. 23 (2000) 285.
[8] Z. Guo, S. Vangapandu, R.W. Sindelar, L.A. Walker, R.D. Sindelar, Curr. Med. Chem. 12 (2005) 173.
[9] I.J.C. Vieira, R. Braz-Filho, Stud. Nat. Prod. Chem. 33 (2006) 433.
[10] A.M. Pohlit, V.A.P. Jabor, R.C.d.N. Amorim, E.C. Costa e Silva, N.P. Lopes, J. Braz. Chem. Soc. 20 (2009) 1065.
[11] G. Sarais, M. Cossu, S. Vargiu, P. Cabras, P. Caboni, J. Agric. Food Chem. 58 (2010) 2807.
[12] G. Vitanyi, E. Bihatsi-Karsai, J. Lefler, L. Lelik, Rapid Commun. Mass Spectrom. 11 (1997) 691.

[13] K.L. Chan, C.Y. Choo, H. Morita, H. Itokawa, Planta Med. 64 (1998) 741.
[14] C.-Y. Choo, K.-L. Chan, Planta Med. 68 (2002) 382.
[15] S. Tan, K.-H. Yuen, K.-L. Chan, Planta Med. 68 (2002) 355.
[16] H.W. Wernsdorfer, S. Ismail, L. Chan Kit, K. Congpuong, G. Wernsdorfer, Wien. Klin. Wochenschr. 121 (Suppl. 3) (2009) 23.
[17] H. Morita, E. Kishi, K. Takeya, H. Itokawa, O. Tanaka, Chem. Lett. (1990) 749.
[18] H. Morita, E. Kishi, K. Takeya, H. Itokawa, Y. Iitaka, Phytochemistry 33 (1993) 691.
[19] P.C. Kuo, A.G. Damu, T.S. Wu, Chin. Pharm. J. 55 (2003) 257.
[20] A.P. Bruins, Trac- Trends Anal. Chem. 13 (1994) 37.
[21] S. Zhou, M. Hamburger, J. Chromatogr. A 755 (1996) 189.
[22] E. Razzazi-Fazeli, J. Bohm, W. Luf, J. Chromatogr. A 854 (1999) 45.
[23] M. Jin, Y. Zhu, J. Chromatogr. A 1118 (2006) 111.
[24] W. Buchberger, W. Ahrer, J. Chromatogr. A 850 (1999) 99.
[25] G. Dusi, V. Gamba, J. Chromatogr. A 835 (1999) 243.
[26] D.A. Volmer, C.M. Lock, Rapid Commun. Mass Spectrom. 12 (1998) 157.
[27] K. Huikko, T. Kotiaho, R. Kostiainen, Rapid Commun. Mass Spectrom. 16 (2002) 1562.
[28] B. Law, D. Temesi, J. Chromatogr. B 748 (2000) 21.
[29] K.S. Hakala, L. Laitinen, A.M. Kaukonen, J. Hirvonen, R. Kostiainen, T. Kotiaho, Anal. Chem. 75 (2003) 5969.
[30] N.B. Cech, J.R. Krone, C.G. Enke, Anal. Chem. 73 (2000) 208.
[31] J.M. Cha, S. Yang, K.H. Carlson, J. Chromatogr. A 1065 (2005) 187.
[32] S. Ding, E. Dudley, S. Plummer, J. Tang, R.P. Newton, A.G. Brenton, Rapid Commun. Mass Spectrom. 20 (2006) 2753.
[33] C. Zhao, C. Li, Y. Zu, J. Pharm. Biomed. Anal. 44 (2007) 35.